Synthesis of PS/PMMA Core−Shell Structured Particles by Seeded Suspension Polymerization

Odinei H. Gonçalves, José M. Asua, Pedro Henrique Hermes de Araújo,* and Ricardo A. F. Machado

Laboratório de Controle de Processos, Universidade Federal de Santa Catarina, CP 476, CEP 80010-970, Florianópolis-SC, Brazil, and Institute for Polymer Materials "POLYMAT" and Grupo de Ingeniería Química, Departamento de Química Aplicada, Facultad de Ciencias Químicas, University of the Basque Country, Apdo. 1072, 20080 Donostia-San Sebastián, Spain

Received March 28, 2008; Revised Manuscript Received July 7, 2008

ABSTRACT: The synthesis of large core−shell particles suitable for applications as rigid foams is reported by means of a seeded suspension polymerization. Suspension polystyrene particles were used as a seed and methyl methacrylate as second stage monomer. Structured particles with a core of polystyrene and a shell composed by PMMA domains densely dispersed in a polystyrene matrix were obtained. The size and concentration of these domains (shell) decreased from the outer shell to the core of the particle. The particle morphology was largely controlled by the limitations to the diffusion of the MMA through the polymer particle. Therefore, increasing the swelling time resulted in a higher amount of PMMA incorporated and in a higher shell thickness. The effect of the initiator was relatively minor. The molecular weights of shell polymer were substantially higher than those of the PMMA obtained through standard batch and semibatch suspension polymerization.

Introduction

Suspension polymerization is a process in which the polymerization of relatively water-insoluble monomer droplets formed by vigorous stirring in the presence of a steric stabilizer leads to an aqueous dispersion of polymer particles. Suspension polymerization is employed in the production of several important commercial resins as poly(vinyl chloride), acrylate copolymers, and styrene copolymers, such as expandable polystyrene (EPS), acrylonitrile−butadiene−styrene resin (ABS), and styrene−acrylonitrile resin (SAN). Excellent reviews of the process are available.[1−6]

The main applications of the EPS foams are in thermal insulation and in the packaging sector. The range of applications of these foams would be enlarged by improving the properties of EPS rigid foams, in particular their chemical resistance. In the case of EPS, the polymer beads are impregnated with a blowing agent before the end of the polymerization and after polymerization are molded without any postprocessing step. Therefore, any attempt to change the chemical properties of the polymer beads should be done at the polymerization reactor.

Core−shell morphology is of particular interest because particles with a composition profile along their radius could present unique properties. Thus, for the suspension-made EPS, a core−shell morphology of the polymer beads could be a suitable strategy to improve the chemical resistance of the foam because a shell composed by a polymer more resistant than polystyrene to organic solvents could improve the resistance of the entire foam sheet. The production of particles with complex morphology have been extensively studied[7−14] in the past few decades in systems such as emulsion and dispersion polymerization. However, just a few works can be found on suspension polymerization.[15−20] Suspension particles formed by a liquid hydrocarbon core and a rigid cross-linked shell mostly composed by acrylonitrile and methacrylonitrile have been reported.[15−18] When exposed to heat, the shell softens and the hydrocarbon gasifies, causing the expansion of the microsphere. The expanded particles are used in printing inks and textiles.

* To whom correspondence should be addressed. E-mail: pedro@enq.ufsc.br.

Table 1. Formulation Used for the Core−Shell Synthesis

reactant	weight (g)
water	560.00
polystyrene seed	197.40
methyl methacrylate	62.00
benzoyl peroxide	0.223/0.341
poly(vinylpyrrolidone)	1.980
ascorbic acid	0.789

The process is restricted to particles with diameters lower than 20 μm and liquid cores and a single polymer shell. Lenzi et al.[19] used a semibatch emulsion/suspension polymerization hybrid system to obtain particles formed by a suspension-like core and a shell composed by aggregated emulsion particles. The resulting particles presented high surface area and broad molecular weights distribution and can be used as support for catalysts. However, the particles did not present a smooth spherical shape. Although not reported, the presence of high concentrations of emulsifier characteristic of emulsion polymerization would provide water sensitivity to the material and likely a substantial amount of emulsion particles remained in the aqueous phase. Byun et al.[20] used polystyrene beads (diameters from 35 to 75 μm) obtained by suspension polymerization and treated with ozone gas to introduce hydroperoxide groups onto the surface. After that, PMMA chains were grafted onto the surface of the PS beads, yielding core−shell particles suitable to be used in biomedical applications for immobilization of proteins and cells. The ester groups of the grafted PMMA were reduced to hydroxyl groups with lithium aluminum hydride. After adding ethylene oxide to the hydroxyl groups, PS-sg-PEG beads with diameters from 80 to 150 μm were obtained. Although large particles can be produced (diameters up to 100 μm), graft efficiency is low due to excessive secondary particles formation. None of these particles can be used as rigid foams.

In this work, the synthesis of PMMA/PS structured core−shell particles useful for application as rigid foams is reported. These particles should have a particle size of 400−1600 μm, a spherical shape,[4] and an external shell more resistant to solvents than polystyrene. The idea is to form a poly(methyl methacrylate) shell on suspension-made polystyrene particles. Although

10.1021/ma800693m CCC: $40.75
Published on Web 09/12/2008

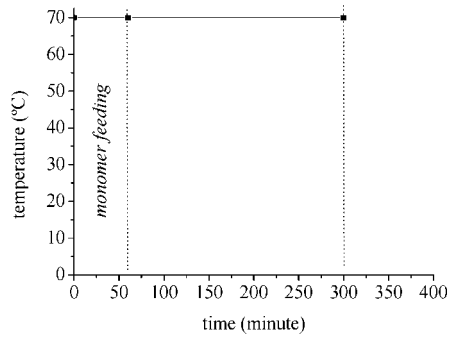

Figure 1. Temperature profile used in the experiment (swelling time = 0 min).

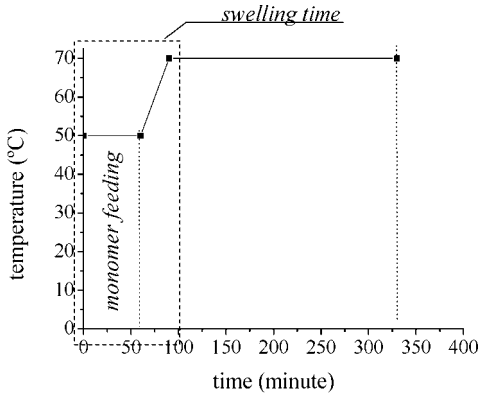

Figure 2. Temperature profile used in the experiment (swelling time = 90 min).

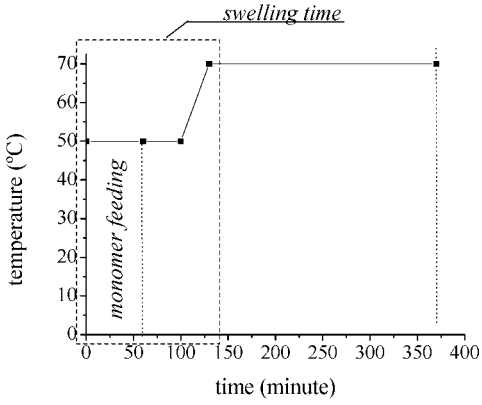

Figure 3. Temperature profile used in the experiment (swelling time = 130 min).

there is plenty of information regarding the mechanisms involved in the development of the morphology of emulsion particles, the difference in size between emulsion and suspension particles (about 4 orders of magnitude) introduces aspects that make of limited use the information available (diffusional limitations to monomer mass transfer; much lower number of particles, which favors the nucleation of secondary particles; much smaller polymer−water interfacial area).

Experimental Section

Materials. Technical grade styrene and methyl methacrylate were used as monomers and benzoyl peroxide (BPO, Sigma-Aldrich) was used as initiator. Distilled water was used as continuous phase and poly(vinylpyrrolidone) (PVP K90, 360 000 g/mol, Sul Polímeros Ltda) as stabilizer. Ascorbic acid (Sigma-Aldrich) was used to avoid inhibition caused by oxygen. All chemicals were used as received. Polystyrene (PS) seeds were obtained by batch suspension polymerization at 90 °C, using BPO ($0.36\%_{wt/monomer\ wt}$) as initiator and PVP ($1.0\%_{wt/water\ wt}$) as stabilizer. Polymer beads were washed and dried. Beads retained between Tyler Standard sieves with nominal apertures of 710 and 1180 μm were used as seed particles in the synthesis of core−shell particles.

Core−Shell Synthesis. The synthesis of core−shell particles was carried out in a 1 L jacketed reactor with a three-bladed propeller stirrer. The formulation employed is presented in Table 1. The initiator concentration was varied in some experiments.

Three synthetic strategies were implemented differing in the way in which the monomer was fed into the system. In all of them, the initial charge was composed by distilled water, polystyrene seeds, PVP, and ascorbic acid. The monomer feed was composed by initiator and MMA, and it was fed to the reactor at a constant rate (0.9 g/min). In the first strategy (Figure 1), the monomer and the initiator were fed when the reactor was at the reaction temperature, 70 °C; after monomer feeding, the system was allowed to react for 4 h. In the second strategy (Figure 2), the monomer and the initiator were fed while the reactor was at 50 °C; when the monomer feeding was finished, the system was heated up to 70 °C and the reaction was carried out for 4 h. Finally, in the third strategy (Figure 3), the monomer and the initiator were fed with the reactor at 50 °C, and after completion of the addition, the system was kept at 50 °C for an additional 40 min and then heated to 70 °C. At 50 °C the decomposition rate of BPO is very low ($t_{1/2} \approx 365$ h at 50 °C); therefore, the period of time in which the system was kept at low temperature before reaching 70 °C ($t_{1/2} \approx 10$ h) was arbitrarily defined as swelling time as no significant amount of PMMA is expected to be formed under these conditions. Applying this definition, in the first strategy the swelling time was zero, since monomer was fed at 70 °C. In the other two strategies, the respective swelling times were 90 and 130 min. Temperature profiles employed in these strategies are illustrated in Figures 1−3.

In all experiments, the monomer/initiator solution was added at a low and constant rate (0.9 g/min) to the reactor in order to avoid a high concentration of monomer in the outer layers of the seed particles that would lead to particle agglomeration as the particle surface becomes very sticky at monomer concentrations between 40% and 60%.[1,2] A trial was made feeding all the monomer to the initial charge at 50 °C, and the seed particles agglomerated almost instantaneously, leading to suspension failure. The ratio methyl methacrylate/polystyrene was limited in the experiments to avoid the breakage of the swelled seed particles by the shear forces inside the reactor.

Standard Batch and Semibatch Suspension Polymerizations. Batch and semibatch methyl methacrylate suspension polymerization were carried out in order to evaluate the effect of the polystyrene seed on the molecular weights. Reactions without seeds employed the same reaction setup (1 L jacketed reactor, three-bladed propeller stirrer) and formulation of the core−shell synthesis presented in Table 1, but no polystyrene seed was used. In batch MMA suspension polymerizations, the initial charge was composed by water, ascorbic acid, and poly(vinylpyrrolidone). The initial charge was heated to 50 °C, and a monomer/initiator solution (benzoyl peroxide at 0.23 mol %) was added to the reactor. After that, temperature was increased to 70 °C, and the stirring rate was set to 900 rpm; the system was allowed to react for 4 h. In semibatch suspension polymerizations, water, ascorbic acid, and poly(vinylpyrrolidone) formed the initial charge of the reactor. The stirring rate was set to 900 rpm, and the system was heated to 70 °C; after that, monomer/initiator solution (benzoyl peroxide at 0.23 mol %) was added at a constant rate (0.9 g/min). After completion of the addition, the system was allowed to react for 4 h.

Characterization. Polymer composition was determined by ^{1}H NMR using deuterated chloroform as diluent. The spectra were recorded at 20 °C using a Bruker Avance spectrometer (500 MHz). The molar percentage of poly(methyl methacrylate) in the sample was determined by the peak of CH_3−O group (at 3.6 ppm) and the peaks characteristic of the aromatic ring of the polystyrene (between 7.2 and 6.2 ppm). The peaks of the CH_2 and CH groups were used to verify the integration error. The efficiency of incorporation was

Table 2. Concentration of PMMA−Shell Polymer and Efficiency of Incorporation (BPO Concentration of 0.23 mol %)

swelling time (min)	PMMA−shell polymer (mol %)	efficiency of incorporation (%)
0	3.0	11
90	9.0	38
130	23.0	97

defined as the ratio of the MMA fed to the reactor and the MMA effectively incorporated to the particles.

Transmission electron microscopy (Hitachi 7000 at 75 kV) was used to study the morphology of the particles; the images were taken at 6000× magnification. Particles were sliced using an ultramicrotome and deposited on a copper grid; then, the samples were stained by ruthenium tetroxide (RuO_4) vapor for 1 h (PS appears dark whereas PMMA appears light). Particle morphology was also analyzed by FTIR of the cross-sectioned particles.

Composition mapping was carried out with Fourier transform infrared spectroscopy (FTIR). A Nicolet 5DXC spectrometer was used with an optical microscope, and the particles were sliced with an ultramicrotome to obtain cross section with 1 μm thickness. They were deposited on KBr tablets before analysis, and the peak at 1740 cm^{-1} was used to determine the presence of PMMA.

Molecular weight distributions were measured by size exclusion chromatography (SEC). SEC was performed using a Waters apparatus equipped with three Styragel columns in series (HR 2, HR 4, HR 6; effective molecular weight ranges of $5 \times 10^2-2 \times 10^4$, $5 \times 10^3-6 \times 10^5$, and $2 \times 10^5-1 \times 10^7$ g/g mol, respectively), at 35 °C with tetrahydrofuran (THF) as eluent (flow rate was 1.0 mL min^{-1}). A Waters 2410 refractive index detector was used, and molar masses were determined from a calibration curve based on PS standards (average molecular weights varying from 580 to 11 200 000 g/g mol). PMMA (shell polymer) was separated from PS (core polymer) before SEC analysis. A sample of the core−shell particles was dissolved in THF; after complete dissolution, cyclohexane was slowly added until PMMA precipitation occurs. The precipitate was separated by sedimentation and dried; after that, it was dissolved in acetic acid to separate any trace of polystyrene. The fraction soluble in acetic acid was filtered and dried. Infrared spectra were obtained from the PMMA and PS fractions to ensure that each fraction was composed of pure polymer. Peaks at 700 and 750 cm^{-1} were used to identify the presence of polystyrene, while the peak at 1740 cm^{-1} was used for PMMA. For all samples, IR spectra confirmed that the separation procedure was successful and that the polymer fractions were pure.

The monomer conversion curve was determined gravimetrically in ampules at 70 °C, using benzoyl peroxide (at 0.23 mol %), and the same MMA/seed particles mass proportion used in core−shell synthesis. At certain times, polymerization was stopped with *p*-benzoquinone (used as inhibitor), and the samples were dried at 60 °C.

Results and Discussion

Shell Formation. The total amount of MMA incorporated into the seed particles with 0.23% of BPO is presented in Table 2. In addition, Figures 4−9 present the particle morphology achieved when the swelling time increased from 0 to 130 min. These figures combined TEM micrographs (Figures 4, 6, and 8) with IR data of the cross section of the particles (Figures 5, 7, and 9).

Each image in TEM micrographs corresponds to the approximate position in the particle diameter marked in Figures 4a, 6a, and 8a. In Figure 5, the cross section of the particle was scanned with IR starting in position P1, which is near the particle surface, passing through the center of the particle (at P4 and P5) and reaching the other side of the cross section at P8; the same is valid for Figures 7 and 9.

Analyzing these data is worth reminding that the solubility of BPO in water is very small[21] (3×10^{-4} g/100 g_{water}) and that it was fed dissolved in the monomer. Comparison of Figures 4, 6, and 8 with Figures 5, 7, and 9 shows that TEM morphologies agreed very well with those determined by IR mapping. IR spectra presented in Figures 5, 7, and 9 confirmed that PMMA concentration was not uniform along the particle radius. PMMA concentration, denoted by the intensity of carbonyl absorption bands at 1740 cm^{-1}, reached maximum values near the particle surface and decreased along the particle radius. TEM images show that the PMMA was distributed

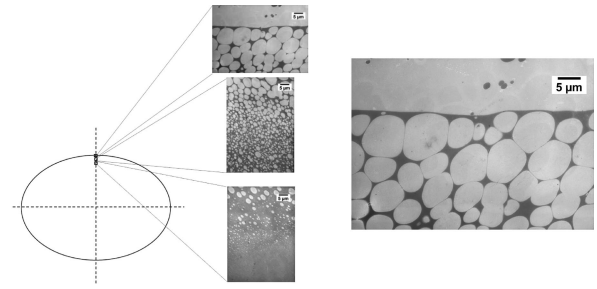

(a) Cross-section representation. **(b)** Detail of the outer region.

Figure 4. TEM images and the approximated representation of the cross section of a typical core−shell particle obtained with swelling time of 0 min and 0.23 mol % of BPO (PMMA appears as light gray and PS as dark gray; 6000×).

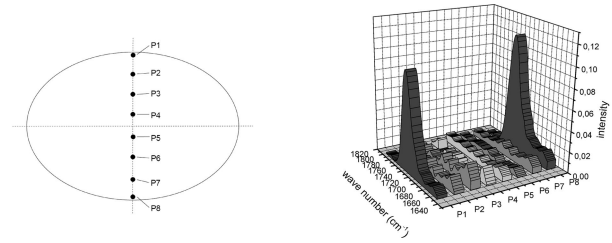

(a) Diagram of the cross-section of the particle showing the positions where spectra were taken. **(b)** Spectra detailing the absorption region characteristic of the PMMA carbonyl group.

Figure 5. FTIR spectra of the cross section of a core−shell particle (70 °C; BPO concentration = 0.23 mol %; swelling time = 0 min).

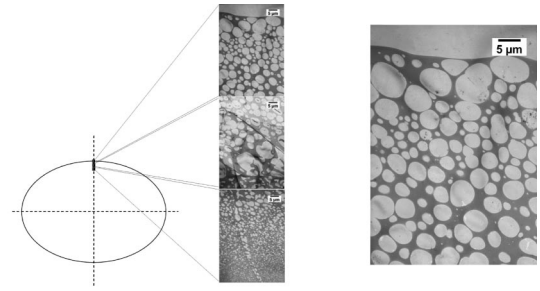

(a) Cross-section representation. **(b)** Detail of the outer region.

Figure 6. TEM images and the approximated representation of the cross section of a typical core−shell particle obtained with swelling time of 90 min and 0.23 mol % of BPO (PMMA appears as light gray and PS as dark gray; 6000×).

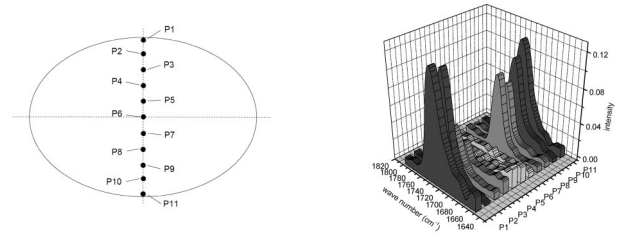

(a) Diagram of the cross-section of the particle showing the positions where spectra were taken. **(b)** Spectra detailing the absorption region characteristic of the PMMA carbonyl group.

Figure 7. IR spectra of the cross section of a core−shell particle (70 °C; BPO concentration = 0.23 mol %; swelling time = 90 min).

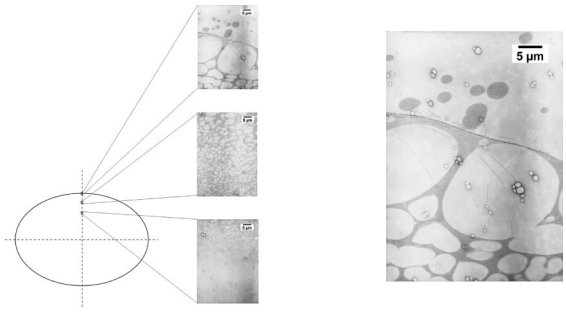

(a) Cross-section representation (6.000X). **(b)** Detail of the outer region.

Figure 8. TEM images and the approximated representation of the cross section of a typical core−shell particle obtained with swelling time of 130 min and 0.23 mol % of BPO (PMMA appears as light gray and PS as dark gray; 6000×).

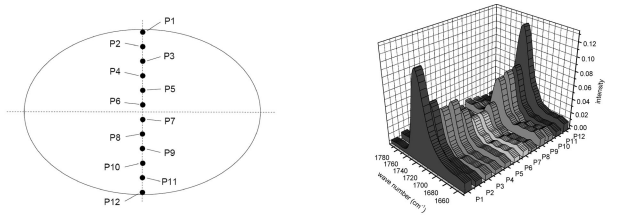

(a) Diagram of the cross-section of the particle showing the positions where spectra were taken. **(b)** Spectra detailing the absorption region characteristic of the PMMA carbonyl group.

Figure 9. IR spectra of the cross section of a core−shell particle (70 °C; BPO concentration = 0.23 mol %; swelling time = 130 min).

forming domains within the polystyrene matrix. These domains resulted from the phase separation of the PS and the newly formed PMMA because these two polymers are incompatible.

When no swelling time was allowed, Figures 4 and 5 show that a sharp core−shell morphology was obtained, namely only the outer layers of the particle contained PMMA. When the swelling time was increased to 90 min, the shell became thicker, but still the core of the particle was essentially free from PMMA. 130 min of swelling led to a less defined morphology with a continuous decrease of the PMMA concentration from the surface to the center of the particle. After initiator and monomer enter the seeds, diffusion toward the center of the particle and polymerization occur simultaneously. With increasing swelling time, more time is available to monomer/initiator to diffuse before polymerization, resulting in a thicker shell.

Table 2 shows that the swelling time severely affected the fraction of PMMA incorporated into the polymer particles and that long swelling times (130 min) were required to achieve the incorporation of almost all the MMA. When no swelling time was used (meaning that the monomer was added at the polymerization temperature), only a thin shell was obtained and most of the monomer polymerized before entering the seed particles.

Figure 10 presents the evolution of monomer conversion in the bulk polymerization carried out with the same monomer/initiator/seed ratio. It can be seen that monomer conversion reached high conversion in 40−50 min. The combination of this piece of information with the particle morphologies shown in Figures 4−9 leads to the conclusion that the rate of diffusion of the monomer through the polymer particles played a critical role in determining the morphology of the particles. As the polymerization was faster than monomer diffusion, well-defined core−shell structure (high concentration of PMMA at the shell and no PMMA at the core) were obtained when no or short swelling times were used. However, this resulted in a substantial polymerization in the aqueous phase namely in a less efficient incorporation.

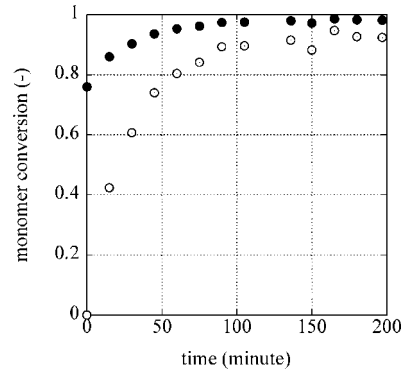

Figure 10. Bulk polymerization in ampule showing (○) monomer conversion and (●) total polymer fraction (70 °C; BPO concentration = 0.23 mol %; seed/MMA = 3.2:1).

Table 3. PMMA−Shell Polymer Concentration and Efficiency of Incorporation

BPO concentration (mol %)	PMMA−shell polymer (mol %)	efficiency of incorporation (%)
0.15	9.4	40
0.23	9.0	38

It is also worth noting that in all cases it was not obtained a well-defined core−shell morphology (Figures 4, 6, and 8) as the surface of the particles was composed by polystyrene with PMMA domains below the surface. This kind of morphology was obtained because the system was not under thermodynamic equilibrium as the polymerization rate is much faster than the diffusion of PMMA/MMA in the swollen seed particles. This resulted in the formation of PMMA domains close to the surface of the particle instead of a continuous PMMA shell.

Influence of Initiator Concentration. One would expect that lowering the rate of polymerization would result in a more efficient incorporation for a given swelling time. Therefore, the amount of initiator was reduced to 0.15 mol % using 90 min as swelling time. Table 3shows the effect of the initiator concentration on the amount of MMA incorporation into the seed particles for a swelling time of 90 min. Figure 11 shows TEM images of the cross section of a core−shell particle synthesized with 0.15 mol % of BPO, and Figure 12 presents the IR mapping.

Table 3 shows that the incorporation of MMA in the particles was only slightly affected by the initiator concentration. In addition, Figures 7 and 11 show that the profile of concentration of PMMA inside the particles was not significantly affected by the initiator concentration. It is also possible to note in Figure 11 that the decrease of initiator concentration led to an increase in the size of the PMMA domains. This result could be explained by the nucleation rate of PMMA domains that should be

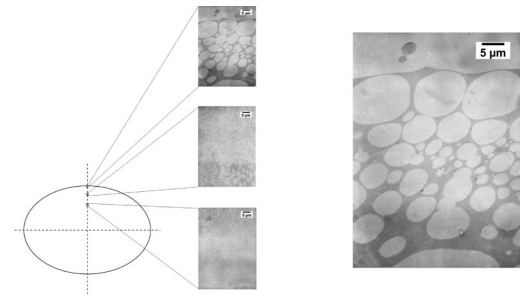

(a) Cross-section representation (6.000X). **(b)** Detail of the outer region.

Figure 11. TEM images and the approximated representation of the cross section of a typical core−shell particle obtained with swelling time of 90 min and 0.15 mol % of BPO (PMMA appears as light gray and PS as dark gray; 6000×).

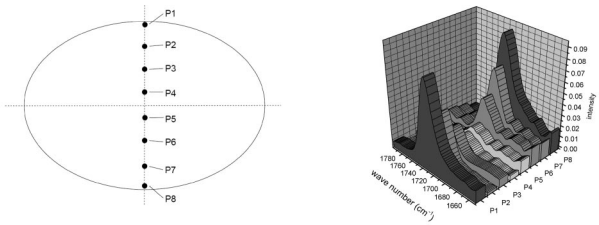

(a) Diagram of the cross-section of the particle showing the positions where spectra were taken.

(b) Spectra detailing the absorption region characteristic of the PMMA carbonyl group.

Figure 12. IR spectra of the cross section of a core−shell particle (70 °C; BPO concentration = 0.15 mol %; swelling time = 90 min).

Table 4. Average Molecular Weights of the PMMA

	M_n ($\times 10^{-3}$ g/g mol)	M_w ($\times 10^{-3}$ g/g mol)	polydispersity
shell polymer, 0.15% BPO	1606	3707	2.0
shell polymer, 0.23% BPO	1387	3086	2.2
batch suspension, 0.23% BPO	265	645	2.4
semibatch suspension, 0.23% BPO	248	670	2.7

expected to increase with increasing radical formation due to initiator decomposition (higher radical concentration leading to higher nucleation rate of PMMA domains).

Average Molecular Weights. Table 4 presents number (M_n) and weight (M_w) average molecular weights and polydispersity of the PMMA formed in the seed particles after the core−shell syntheses (70 °C and swelling time of 90 min) with 0.15% and 0.23% BPO. The values were compared to standard batch MMA suspension polymerization (70 °C and 0.23% BPO) and standard semibatch suspension polymerization (monomer feed rate of 0.9 g/min, 70 °C and 0.23% BPO).

Table 4 shows that the polymer formed in standard batch and semibatch polymerizations presented very similar values of average molecular weights. This result could be expected as no polymer seed was present at the initial charge of the semibatch reaction, and similar monomer and initiator concentrations profiles may be found on both reactions as the initiator was fed with the monomer to the reactor. On the other hand, the PMMA that formed the shell (namely, the fraction polymerized inside the seeds) had higher molecular weights. This was likely due to the high viscosity of the monomer swollen particle, which limited the mobility of the growing chains decreasing their termination rate (gel effect) and increasing molecular weights.

Conclusions

Core−shell particles of sizes suitable for rigid foams were obtained by seeded suspension polymerization of methyl methacrylate using polystyrene particles as seeds. The particles presented a complex morphology with a polystyrene core and a shell composed by PMMA domains distributed in the polystyrene matrix.

Shell thickness and the amount of MMA incorporated as a polymeric shell to the seed particles were strongly influenced by the strategy adopted for monomer feeding into the system: the higher the swelling time, the higher both the shell thickness and the fraction of PMMA formed inside the seeds as a shell. However, the less sharp the interface between the core and the shell.

The decrease in the initiator concentration led to an increase in the size of the PMMA domains inside the core−shell particles. Nevertheless, the fraction of methyl methacrylate and the shell thickness were only slightly affected by initiator concentration. These results indicate that the monomer and initiator diffusion to the seed particles plays a key role on the efficiency of monomer incorporation.

Molecular weight of PMMA in the core−shell particles was 5 times higher than molecular weight of the PMMA obtained in standard batch suspension polymerization due to the high polymer concentration and diffusional limitations (gel effect) that took place from the beginning of the reaction decreasing the termination rate.

Acknowledgment. The authors thank CNPq (Conselho Nacional de Desenvolvimento Científico e Tecnológico), CAPES (Coordenação de Aperfeiçoamento de Pessoal de Nível Superior), and FINEP (Financiadora de Estudos e Projetos) for the financial support as well as the Programme Alban, the European Union Programme of High Level Scholarships for Latin America, scholarship no. E06D101711BR.

References and Notes

(1) Yuan, H. G.; Kalfas, G.; Ray, W. H. *Macromol. Sci., Rev. Macromol. Chem. Phys.* **1991**, *C31*, 215–299.
(2) Vivaldo-Lima, E.; Wood, P. E.; Hamielec, A. E.; Penlidis, A. *Ind. Eng. Chem. Res.* **1997**, *36*, 939–965.
(3) Dowding, P. J.; Vincent, B. *Colloids Surf., A* **2000**, *161*, 259–269.
(4) Scheirs, J.; Priddy, D. B. *Modern Styrenic Polymers: Polystyrenes and Styrenic Copolymers*; Wiley Series in Polymer Science; John Wiley & Sons: Chichester, 2003.
(5) Brooks, B. W. Free-radical Suspension Polymerization. In *Handbook of Polymer Reaction Engineering*; Meyer, T., Keurentjes, J., Eds.; Wiley-VCH: Weinheim, 2005.
(6) Kotoulas, C.; Kiparissides, C. Suspension Polymerization. In *Polymer Reaction Engineering*; Asua, J. M., Ed.; Blackwell Publishing: Oxford, 2007.
(7) Rajatapiti, P.; Dimonie, V. L.; El Aasser, M. S.; Vratsanos, M. S. *J. Appl. Polym. Sci.* **1997**, *63*, 205–219.
(8) González-Ortiz, L. J.; Asua, J. M. *Macromolecules* **1995**, *28*, 3135–3145.
(9) González-Ortiz, L. J.; Asua, J. M. *Macromolecules* **1996**, *29*, 383–389.
(10) González-Ortiz, L. J.; Asua, J. M. *Macromolecules* **1996**, *29*, 4520–4527.
(11) Herrera, V.; Pirri, R.; Leiza, J. R.; Asua, J. M. *Macromolecules* **2006**, *39*, 6969–6974.
(12) Keusch, P.; Williams, D. J. *J. Polym. Sci., Part A: Polym. Chem.* **1973**, *11*, 143–162.
(13) Lee, D. I.; Ishikawa, T. *J. Polym. Sci., Part A: Polym. Chem.* **1983**, *21*, 147–154.
(14) Morgan, L. W. *J. Appl. Polym. Sci.* **1882**, *27*, 2033–2042.
(15) Ali, M. M.; Stover, H. D. H. U.S. Patent 6,828,025, **2004**.
(16) Kasai, Y. K.; Hattori, A. M.; Takeuchi, H.; Sakurai, N. U.S. Patent 4,798,691, **1989**.
(17) Kawaguchi, Y.; Itamura, Y.; Onimura, K.; Oishi, T. *J. Appl. Polym. Sci.* **2005**, *96*, 1306–1312.
(18) Kolarz, B. N.; Trochimczuk, A. W.; Wojaczynska, M.; Drewniak, M. *Angew. Makromol. Chem.* **2003**, *217*, 19–29.
(19) Lenzi, M. K.; Silva, F. M.; Lima, E. L.; Pinto, J. C. *J. Appl. Polym. Sci.* **2003**, *89*, 3021–3038.
(20) Byun, J.; Kim, J.; Chung, W.; Lee, Y. *Macromol. Biosci.* **2004**, *4*, 512–519.
(21) Alduncin, J. A.; Forcada, J.; Asua, J. M. *Macromolecules* **1994**, *27*, 2256–2261.

MA800693M